Mine Water and the Environment (2021) 40:174–188
https://doi.org/10.1007/s10230-020-00725-3

TECHNICAL ARTICLE

Influences of Tailings Particle Size on Overtopping Tailings Dam Failures

Chi Yao[1,3] · Ligong Wu[1,3] · Jianhua Yang[1,3] · Lixing Xiao[1,3] · Xiaofeng Liu[2,3] · Qinghui Jiang[1,3] · Chuangbing Zhou[1,3]

Received: 7 October 2019 / Accepted: 17 September 2020 / Published online: 14 October 2020

Abstract

A series of physical tests were carried out using three different particle sizes to investigate the influence of tailings size on the failure process of a tailings dam subjected to overtopping. In addition, the overtopping failure process was simulated with a computational fluid mechanics model. The tests results showed that with increased tailings size, the mode of failure gradually changed from undercut erosion to surface scouring, while the gully cut by the water had a greater width to depth ratio. In addition, the particle size also affected the characteristics of the discharge process and its duration. Numerical simulation results were basically consistent with the physical model results with respect to both discharge process and duration time. The comparison shows that the numerical method could possibly be useful for other studies on the overtopping failure of tailings dams.

Keywords Physical test · Numerical simulation · Undercut erosion · Surface scouring

Introduction

Tailings ponds are built from the tailings that accumulate during mining. Due to their low cost, tailings dams are the main method used to dispose of tailings. The proper construction and maintenance of tailings ponds determines whether mine production and construction can proceed smoothly, and whether the people, property, and the surrounding environment downstream of the dam will be safe (Fourie et al. 2010). Most tailings ponds in China adopt the upstream damming method, even though this technology is being abandoned in many mining countries because of the risks involved, and most of the tailings ponds are located in mountainous areas. Heavy rainfall can cause the water surface to rise in the reservoir, leading to the dam bursting from water flowing over the top of the tailings dam. Thirty eight dam-break accidents occurred in China from 2001 to 2015, and flood overtopping was responsible for 37% of them (Rico et al. 2008). As mining technology has improved, the particle size of tailings has getting smaller and smaller, and tailings dams with different particle sizes show different failure characteristics during a dam break.

Based on empirical analysis, some scholars have proposed that scarp erosion causes overtopping dam failures (Hanson et al. 1999; Ralston 1987), but it is generally impossible to get valid historical data, or to obtain accurate physical and mechanical parameters of the tailings pond (Rico et al. 2008). Since empirical relationships do not describe the dam collapse process well, some scholars began to use physical models and numerical simulation methods to analyze and study the collapse process (Jeyapalan et al. 1983; Tabri et al. 2008; Yin et al. 2011). Through physical experiments, the distribution of downstream tailings particles and the change of a dam's phreatic level can be understood, which is important in designing tailings ponds (Yin et al. 2011). A dam's degree of saturation greatly affects its sliding displacement, and after a dam fails, the degree of damage is related to the amount of erosion of the spillway. Physical models have been used to analyze such aspects and potential corresponding measures to reduce tailings reservoir disasters (Sun et al. 2012). Physical models

Electronic supplementary material The online version of this article (https://doi.org/10.1007/s10230-020-00725-3) contains supplementary material, which is available to authorized users.

✉ Jianhua Yang
yangjianhua86@ncu.edu.cn

[1] School of Civil Engineering and Architecture, Nanchang University, Nanchang 330031, China

[2] China Ruilin Engineering Technology Co., Ltd. Environmental and Safety Affairs Department, Nanchang 330031, China

[3] Jiangxi Key Laboratory of Tailings Reservoir Engineering Safety, Nanchang 330031, China

have also been used to analyze the causes of dam failure, slope stability analysis, and tailings reservoir reinforcement (Deng et al. 2019; Wu et al. 2008, 2018).

At the same time, numerical methods are widely used because of their convenience and low price. Numerical simulation method can simulate the leakage range of tailings sand after a dam failure to determine the extent of the impact of this factor after a dam break (Sun et al. 2014). Numerical simulation methods are increasingly being applied to slope stability and seepage analysis of tailings ponds, which plays an important role in evaluating the stability and safety of tailings ponds (Lyu et al. 2019). In addition, numerical simulation methods are also important in the recurrence and prediction of dam-breaking disasters and to verify the correctness of experiments (Della Vecchia et al. 2019; Schmocker 2009). At present, most research on overflow tailings dam failures have focused on the mechanism of the dam break and the subsequent flow of sediment. Very few researchers have focused on how the size of tailings particles affect an overtopping dam break. In this study, tailings with different particle sizes were used in physical models as dam material, and numerical simulations were conducted to better understand how different particle sizes affect the failure process.

Methods

A size-reduced physical model of a tailings dam failure was constructed according to certain similarity criterion under laboratory conditions (Jing et al. 2019). Tailings with different grain sizes were used to build the dam and water was injected into the reservoir to simulate the process of overtopping. The evolution of the dam failure was observed and recorded with different grain sizes, and the relationship of dam break flow, dam break time, sedimentation beach length, and tailings grain size were analyzed.

Tailings used in the tests were obtained from the #1 tailings dam of the Yongping tailings reservoir of Yongping Copper Mine in Jiangxi Province, China (Fig. 1). There are five dams in this tailings reservoir, and all were constructed using the upstream method. A typical section of the #1 dam was simulated in the model tests.

In designing the model, some reasonable simplifications were made, but in general, physical parameters such as geometry, flow rate, and time are determined according to the Froude similarity criterion (Cui 1991):

$$\lambda_v = \sqrt{\lambda_L} = 1 : 10 \tag{1}$$

$$\lambda_t = \sqrt{\lambda_L} = 1 : 10 \tag{2}$$

$$\lambda_Q = \lambda_L^{5/2} = 1 : 10^5 \tag{3}$$

where: λ_v is the velocity similar scale; λ_t is the time similarity scale; λ_Q is the flow similarity scale; and λ_L is the geometric similarity scale.

Experimental Devices

The physical model dam was constructed at the geometrical scale ratio of 1:100 using the actual ratio of the internal and external slope of the #1 Yongping tailings dam (Fig. 2). The ratio of the outer slope of the #1 dam is 1:4, the slope ratio is 1:15, and the height is 15 cm. The test devices included a test flume 2.4 m × 0.3 m × 0.3 m (length × width × height), with both the upper and the tail end consisting of an unsealed, open glass groove. At one end of the flume is a reservoir for mitigating the impact of water on the dam when it is injected into the glass groove. Flow error in flow control water injection system was controlled within 4% as verified through several measurements using a 1000 mL glass measuring cylinder. A high-speed camera was used to capture the model dam failure process. The tailwater was collected and measured using a 0.59 m × 0.25 m rectangular plastic box with a liquid level display and reading function, and changes in water level were recorded (Fig. 3).

The parameters scale of the physical model was established according to the similarity theory (Table 1). The flow rate in the model test was set to be 0.1 m^3/h, which is consistent with local rainstorm conditions. The injected water flow was kept unchanged during the entire experiment. The dam break was considered completed when the upper and lower gullies that formed were almost unchanged.

Model Materials

Tailings from the Yongping tailings reservoir of Yongping Copper Mine were sieved and divided into three differently sized groups of 0.25–0.5 mm, 0.074–0.25 mm, and < 0.074 mm. Each tailings group were dispersed over 1800 cm^3 to construct the model dam. The particle gradation of the three kinds of tailings was determined by physical experiments in the laboratory, as shown in Fig. 4.

Scanning electron microscope pictures of the copper tailings sand is shown in Supplemental Fig. S-1. As can be seen from Fig S-1(a), for tailings with a particle size of 0.25–0.5 mm, most of the larger particles are columnar with many edges and angles, while most of the smaller particles are granular, and the particles have good contact with each other. By observing the morphology of the surface of the particles at a magnification of 5000×, we found that the surfaces of the particles were clearly layered, well developed,

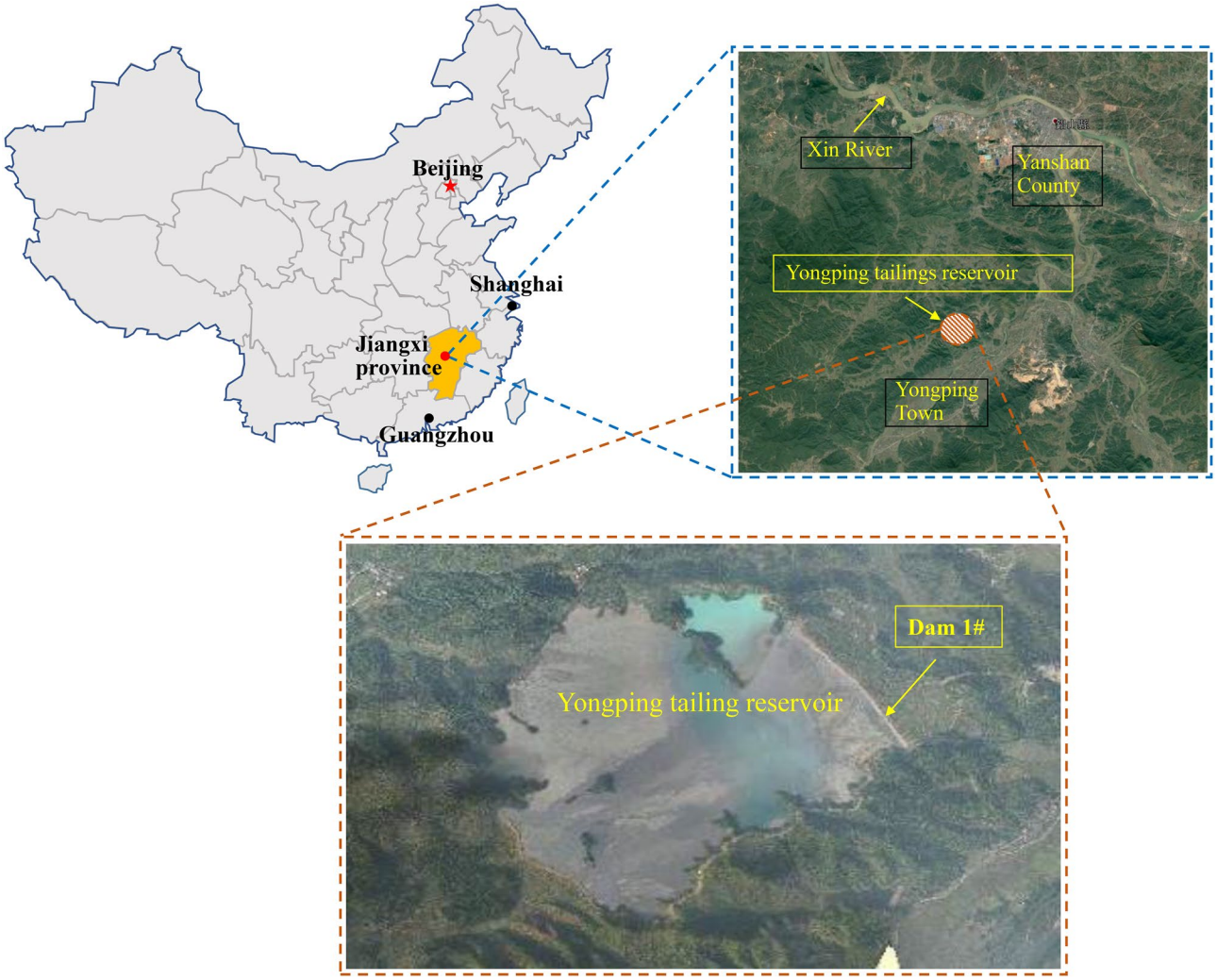

Fig. 1 Location of the Yongping Tailings Reservoir

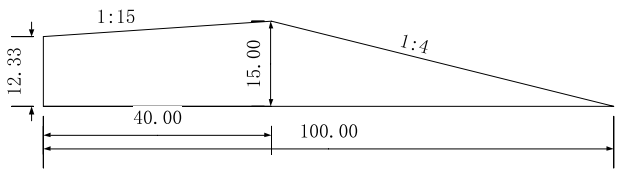

Fig. 2 Section of the physical model dam (unit: cm)

obviously crystallized, and contained a lot of hard, crystalline substances. This morphological feature shows how the loose sediments were dehydrated through consolidation, cementation, recrystallization, and the formation of new minerals into hard sedimentary rock. The surfaces of the particles were rough and there were basically no pores. The contact mode between the particles was a mutual engagement of crystalline substances, and the friction resistance was large.

For the tailings with 0.074–0.25 mm particles (Fig. S-1b), the larger particles were mostly massive, while the smaller particles were mostly granular, with many corners and good contact. At a magnification of 5000×, we found that debris particles of various sizes were attached to the particles and that bedding was developing, but the debris particles had not been converted into crystalline substances, and the hardness was less than in Fig. S-1a. The surface was rough and the friction resistance was large.

For the tailings with a particle size less than 0.074 mm, the particles were uniform and mostly pyramidal. The particles could not be in close contact and were prone to misalignment. At a magnification of 5000×(Fig. S-1c), we found that the surfaces of the particles were smooth, with a layered texture, were prone to flaking, and weaker. There were many clay particles adsorbed to the surfaces of the particles, and the interaction between the clay particles and water improved the shear strength of the tailings.

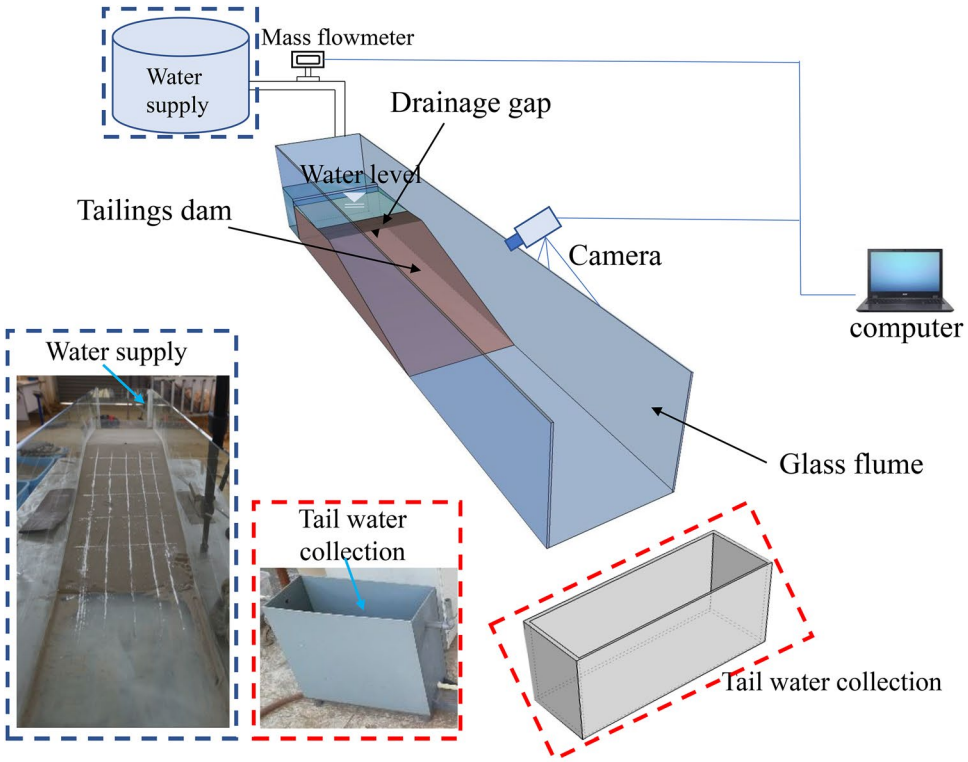

Fig. 3 Schematic diagram of experimental equipment

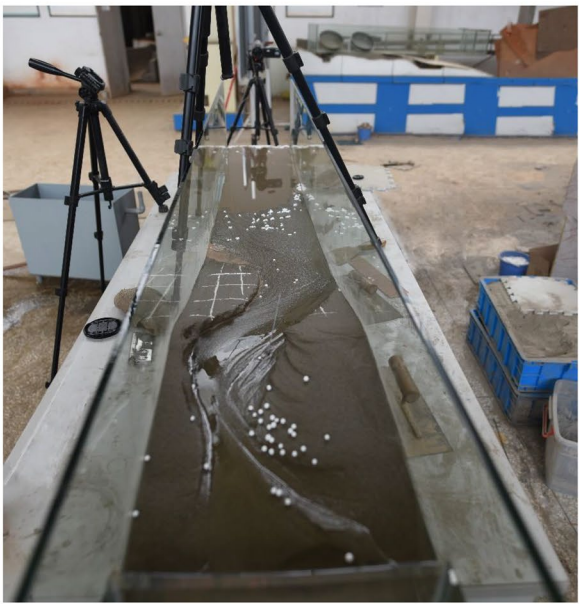

Table 1 Similarity scale of overflow dam failure experiment

Parameter	Similar scale
Geometry	1:100
Velocity	1:10
Time	1:10

Test Results and Analysis

Comparative tests were conducted to examine the effects on different tailings sizes on the overtopping failure process. First, after the construction of the model dam was completed, water was added to the reservoir using the water injection system. When the water level rose to a certain height, it flowed out of the drainage gap set up in advance,

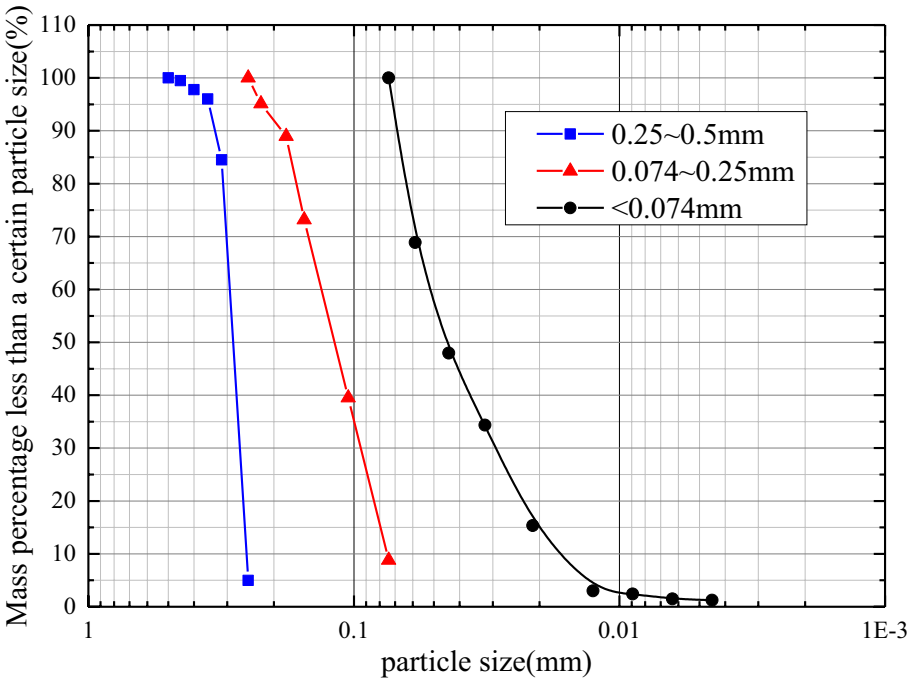

Fig. 4 Gradation curves for three different tailings sizes

and the overtopping failure process was initiated. During the failure process, the failure mode of the dam body was recorded by camera and the tailwater collecting device was used to measure the tailwater flowrate.

Each tailings dam experiment (for each particle size) was repeated three times. Figure 5 compares the states after overtopping failure for each experiment. It can be seen that although the form of the gully was slightly different in the repeated experiments, the dam morphology was basically the same. Therefore, in this paper, one of each group of repeated experiments with different sized tailings was selected as a typical analysis object.

Characteristics of Overtopping Dam Break

After the water level in the reservoir rose to a certain height, the water began to flow over the top of the dam. During the overtopping, a dam body generally experiences several stages: Phase I. Water over the top; Phase II. Initial gully formation; Phase III. Emergence of multi-stage scarps; Phase IV. Widening of the breach until Phase V. Complete failure (Wahl 1998), as shown in Fig. 6. Overtopping failure processes from tests with different tailings sizes are shown in Fig. 7.

We found that for tailings < 0.074 mm, the flow speed of the water was the fastest, the flow was straight, and the wetted area around the flow was relatively small in Phase I, when the water flows over the top of the dam to the toe. In Phase II, the initial gully formed at the toe of the dam started to collapse, but the water surface on the dam body surface was wide, and gully formation was not initially obvious. The dam with these small particles had a continuous multi-level steep ridge that developed continuously during Phase III, which made the gully deeper and deeper. Because of the fine particle size, the tailings behaved similarly to silt and had some viscosity, so the width of the collapsed groove was small, with relatively stable walls.

For the 0.074 ~ 0.25 mm tailings, the permeability of the dam body was enhanced by the larger diameter of the tailings particles, so the wetted area around the water flow increased, and the water surface on the dam body surface was narrower. It took a long time for the water to reach the foot of the dam in Phase I, but the water flow was still straight. As the overtopping water flowed along the dam surface, a small erosion gully formed during Phase II. The middle part of the tailings dam collapsed as the gullies deepened. The surface of the 0.074 ~ 0.25 mm tailings dam had steep ridges, but the gullies formed in Phase III were wider and shallower (Fig. 8).

The still larger tailings particles (0.25 ~ 0.5 mm) weighed more, so as the water flowed, it formed a scour, and the tailings moved down the dam surface for a short distance and then settled on the surface of the dam, which continuously changed the water's flow path, and increased the time for the flow to reach the toe as well as the wetted area. The gully at the top of the dam began to develop as water flowed down the dam surface with difficulty, and there was a continuous collapse where the water flowed through. The water flow path continuously changed until a stable gully formed; as the erosion gully at the top of the dam developed further, the depth increased, and the widest, shallowest gully was produced. The 0.25 ~ 0.5 mm dam did not show steep ridges.

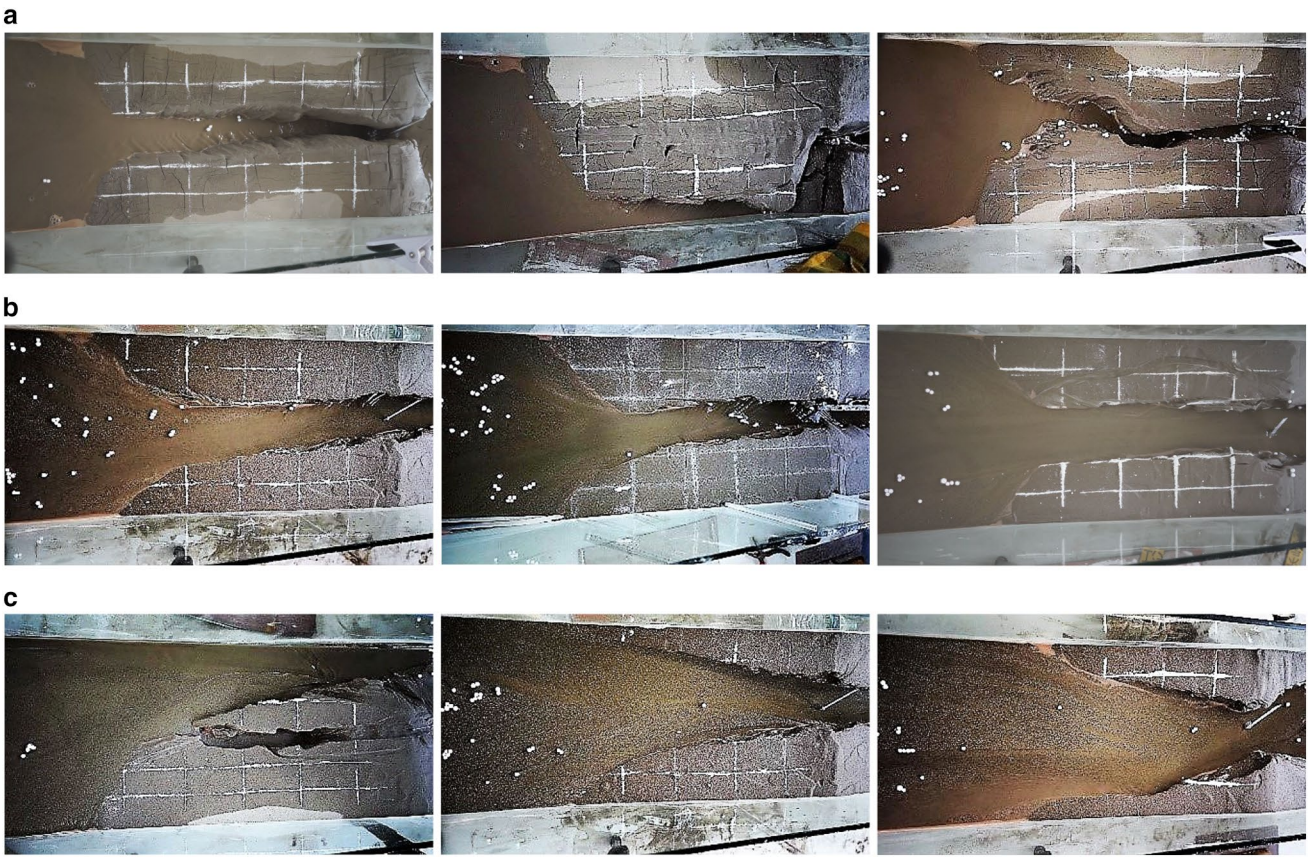

Fig. 5 Comparison of the results of an overtopped dam break **a** tailings < 0.074 mm in repeated tests; **b** tailings between 0.074 ~ 0.25 mm in repeated tests; **c** tailings between 0.25 ~ 0.5 mm in repeated tests

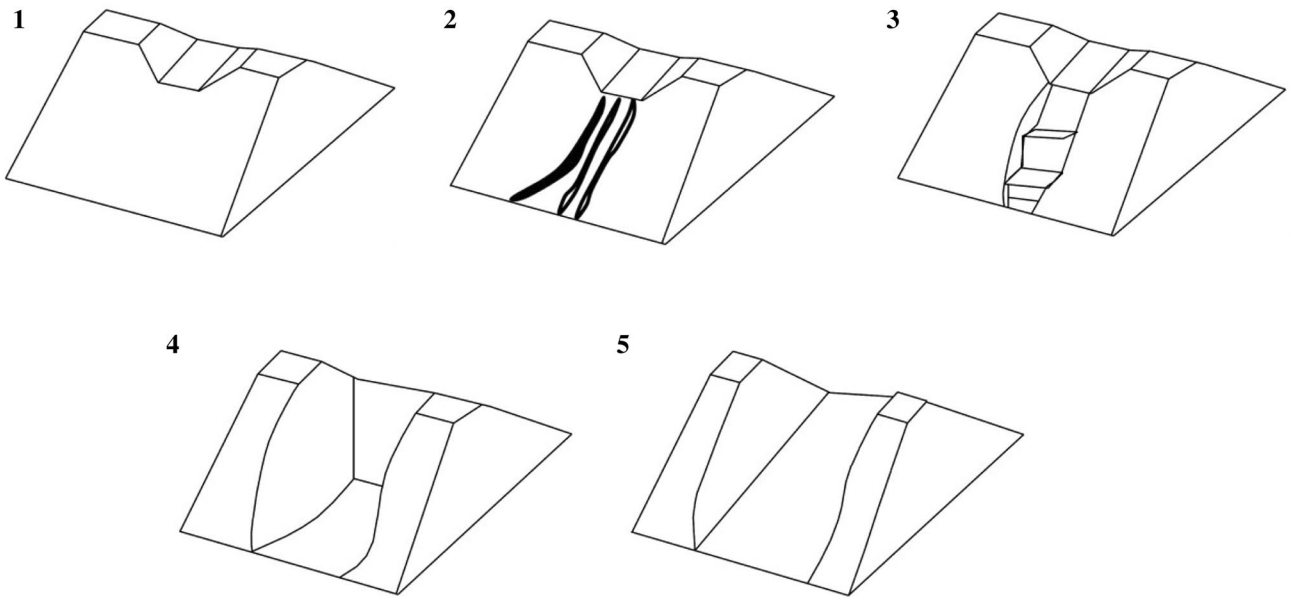

Fig. 6 Phases in the overtopping failure process **a** Phase I; **b** Phase II; **c** Phase III; **d** Phase IV; **e** Phase V

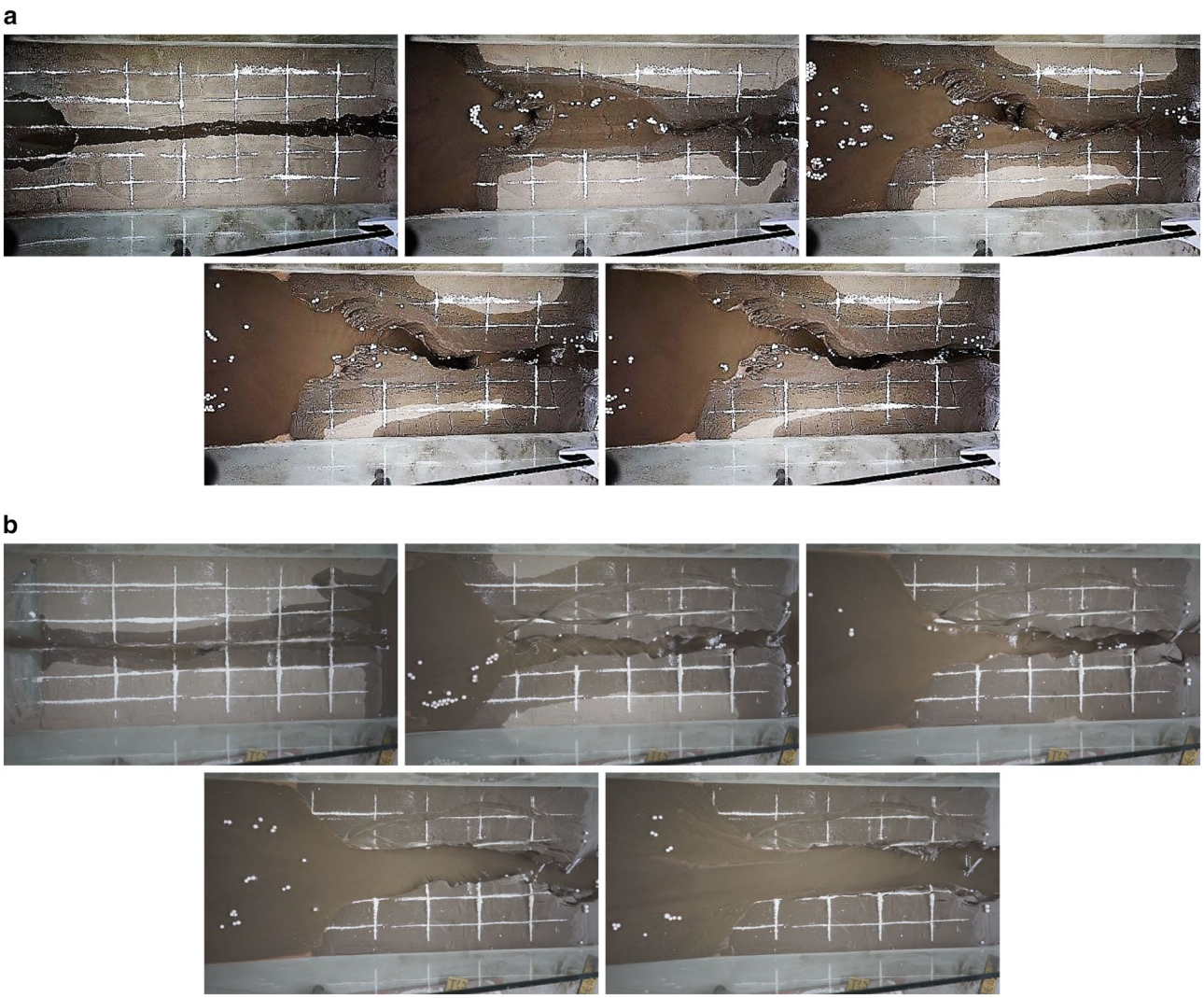

Fig. 7 Failure process for a tailings dam subjected to overtopping **a** with tailings < 0.074 mm; **b** with tailings between 0.074 ~ 0.25 mm; **c** between 0.25 ~ 0.5 mm

As the scarp developed upstream, the depth of the gullies continued to deepen. Due to erosion, the side wall of the gullies gradually became unstable and then collapsed, increasing the width of the gully, and indicating that dam failure had entered Phases IV and V. The start times of each phase for the different particle sizes are shown in Table 2. The dam with the < 0.074 mm tailings formed the deepest, narrowest gully (Supplemental Fig. S-2): the width-depth ratio of the section at the top of the dam was ≈ 5.3 and the shape of the gully was relatively curved. After the dam broke, the amount of tailings discharged from the dam body was minimal.

Compared to the finest size, the gully of the 0.074 ~ 0.25 mm dam was relatively straight, with a width-depth ratio at the dam's top ≈ 1.2; the width of the gully changed little from up to down. The tailings dam body with the coarsest tailings formed the widest and shallowest gully; the width-depth ratio of the section at the top of the dam was ≈ 0.3. The overall shape of the gully was like a horn, wider upstream and narrower downstream.

After the water flowed over the crest, the dam with tailings sized < 0.074 mm was the first to form a small gully. Given the small particle size, destruction of the dam body was mainly due to undercut erosion: the collapse began at the toe of the dam, extended to the middle of the dam, until it finally reached the dam's top. The gully was relatively deep and narrow, and relatively curved. Multi-stage scarps were apparent. As shown in Fig. 9, the course of the width of the breach underwent obvious and abrupt changes.

The dam with the 0.074 ~ 0.25 mm tailings failed via both undercut erosion and surface scouring. After the initial gully formed, the dam began to collapse from the middle. The

Fig. 7 (continued)

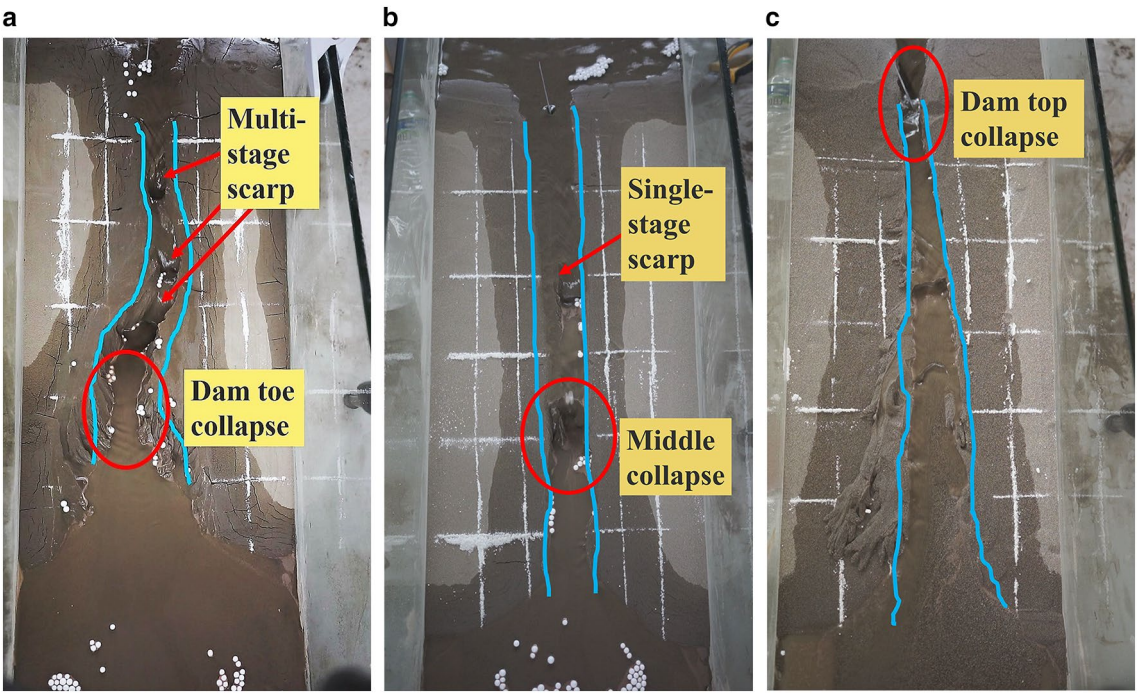

Fig. 8 Overtopping failure patterns with different particle sizes **a** < 0.074 mm; **b** 0.074 ~ 0.25 mm; **c** 0.25 ~ 0.5 mm

gully was relatively straight, and the depth and width were both moderate.

After water overtopped the crest of the dam with tailings between 0.25 ~ 0.5 mm, it started to collapse at the crest, successively followed by a collapse at the middle of the dam and the foot of the dam (Fig. 9). However, due to the large particle size, the dam mainly failed due to surface scouring. Since the tailings accumulating at the top of the dam caused the water flow path to change, more time was needed to form

Table 2 The start time of each phase in the process of tailing dam failuree with different particle sizes(s)

Size (mm)	Phase.I	Phase.II	Phase.III	Phase.IV	Phase.V
< 0.074	2	250	610	900	1314
0.074 ~ 0.25	31	250	390	540	757
0.25 ~ 0.5	130	190	260	380	513

a stable gully. The width of the gully increased from the top of the dam to the toe of the dam, and the final gully was horn-shaped. Water flow eroded both sides of the groove until it collapsed, and the course of the collapsed groove was stepped.

Tailwater Flow

Accurate prediction of flood flow variation is an important basis for dam disaster prevention. In this experiment, the volume of stored water in the reservoir area was 1.602×10^{-3} m^3 before overtopping occurred. The change of flow with time is shown in Fig. 10. As the overtopping occurred, part of the water flow was absorbed by the dam body, but with time, the amount of water absorbed by the dam gradually decreased, so that flow increased over time. The flow of the tailwater was collected and measured after overtopping occurred.

During the entire process of overflow failure, the dam with particles of 0.25 ~ 0.5 mm had the earliest and largest peak flow, which reached 0.035 L/s. The peak flow rate of the dam with particles sized 0.074 ~ 0.25 mm came later and peaked at 0.03 L/s, while the dam with particles less than 0.074 mm had the latest and smallest peak flow (0.028 L/s). Clearly, the coarser the particles were, the more the tailings were scoured by the water flow, which caused the fastest dam break, and largest flow. The converse was also true: the finer the particles were, the slower the dam break, and the flow of the water was less.

Sedimentation Beach Length

After an overtopping dam break, tailings sediment often accumulate at the dam toe. Each sized granule group was tested three times; the measured sedimentation beach lengths are shown in Table 3. The smaller the particle size, the longer the siltation beach, since fine-grained tailings tend

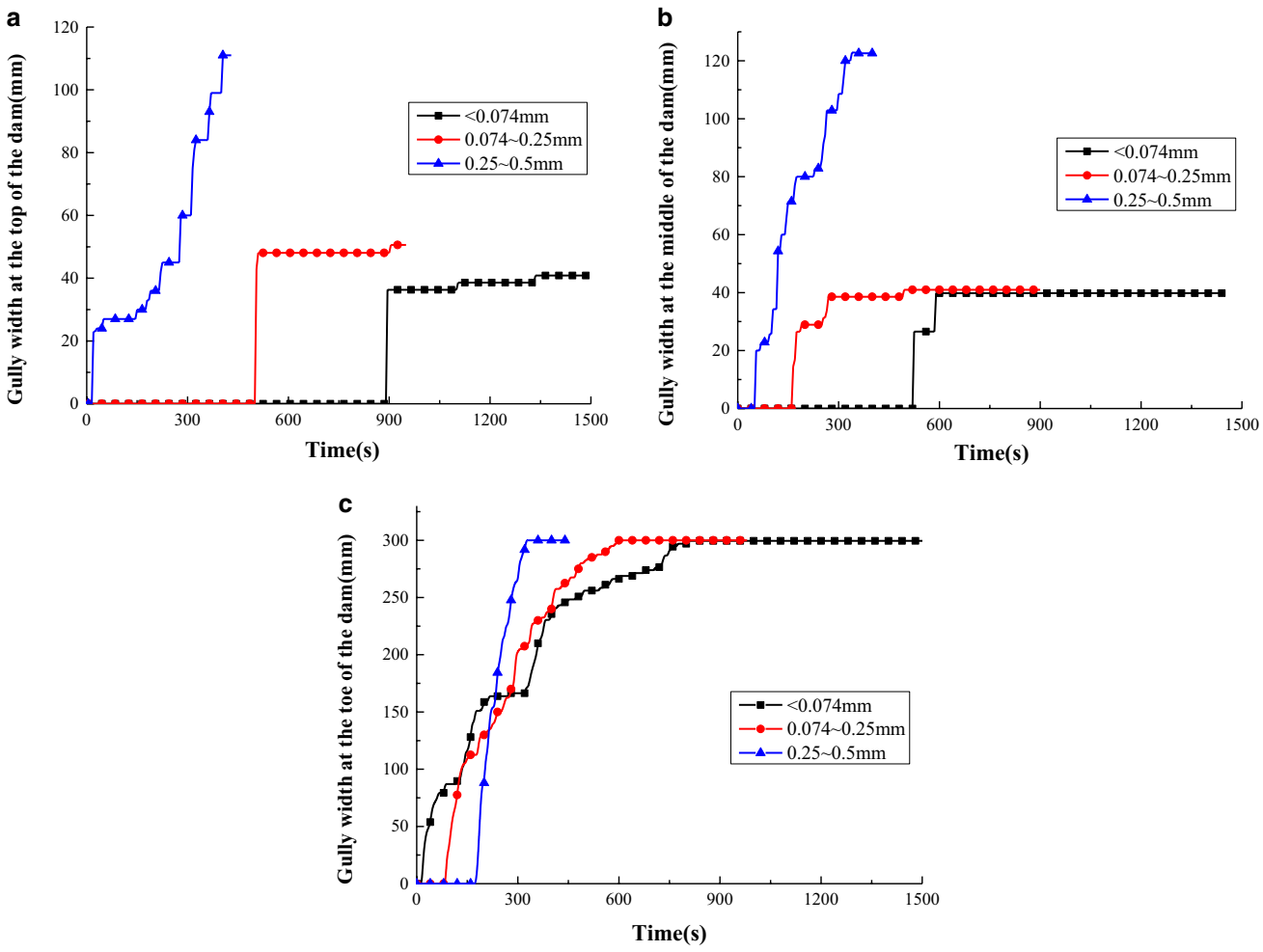

Fig. 9 Comparisons of gully width changes with different particle sizes **a** at the top of the dam; **b** at the middle of the dam; **c** at the toe of the dam

to be carried further by the water, and more of them are suspended. In contrast, the coarser the particle size, the less likely it is that the tailings will be entrained, making the proportion of bed load particles greater, and increasing the surface scouring damage.

As expected, the sized tailings all behaved similarly; at the beginning of the beach, the sediment was mostly composed of larger particles, and with increased distance, the proportion of large particles in the sediment decreased, while the proportion of fine particles increased (Fig. 11). The finer particles moved further in suspension and were deposited only when the flow rate dropped to a very low level.

Numerical Simulation

Numerical Simulation Theory

The computational fluid mechanics software FLOW-3D was used to simulate the failures of the dams with different particle sizes. The sediment scouring module in FLOW-3D is based on sediment theory and the RNG $k-\varepsilon$ model of Mastbergen and Van Den Berg (2003), which can accurately calculate sedimentation, erosion, and movement. The software uses FAVOR technology to divide the computational grid, so that the calculation is more accurate, making it possible to simulate the complex sand water flow state during the dam failure process well. The critical shields coefficient was calculated by the Soulsby-Whitehouse equation (Soulsby 1998), based on the local bed shear stress τ of the riverbed:

$$\theta_i = \frac{\tau}{\|g\|d_i\left(\rho_i - \rho_f\right)} \tag{4}$$

Table 3 Length of sedimentation beach with three particle sizes (m)

Particle size (mm)	Length of sedimentation beach (m)		
	First test	Second test	Third test
< 0.074	0.47	0.46	0.51
0.074 ~ 0.25	0.40	0.38	0.39
0.25 ~ 0.5	0.29	0.30	0.26

The entrainment lift velocity of the sediment is then computed as (Mastbergen and Van Den Berg 2003):

$$u_{lift,i} = \alpha_i n_s d_*^{0.3}\left(\theta_i - \theta'_{cr,i}\right)^{1.5}\sqrt{\frac{\|g\|d_i\left(\rho_i - \rho_f\right)}{\rho_f}} \tag{5}$$

where α_i is the entrainment parameter, and n_s is the outward pointing normal to the packed bed interface.$u_{lift,i}$ is then used to compute the amount of packed sediment that is converted into suspension, effectively acting as a mass source of suspended sediment at the packed bed interface. After that, the sediment is transported with fluid flow, using the turbulence model governing equation (Wilcox 1994).

Numerical Model

As shown in Fig. 12, a small gap was set up at the top of the dam in advance to guide the flow of water so that the overflow dam break would occur in the model calculation area, avoiding the distortion of results that would have been caused by a random breach position.

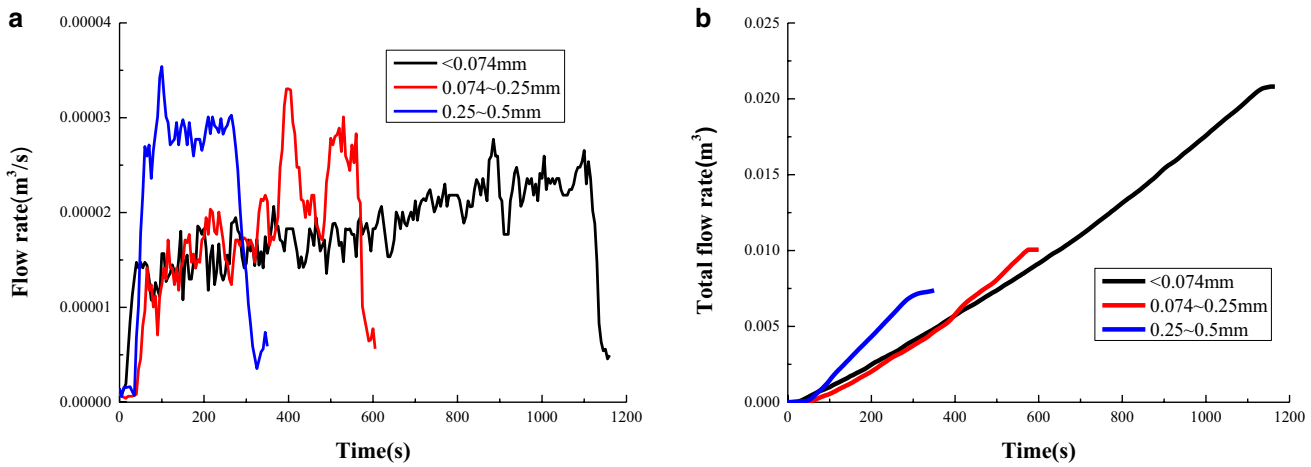

Fig. 10 Comparison of accumulated flow rate from overtopping process for dams with different tailings sizes

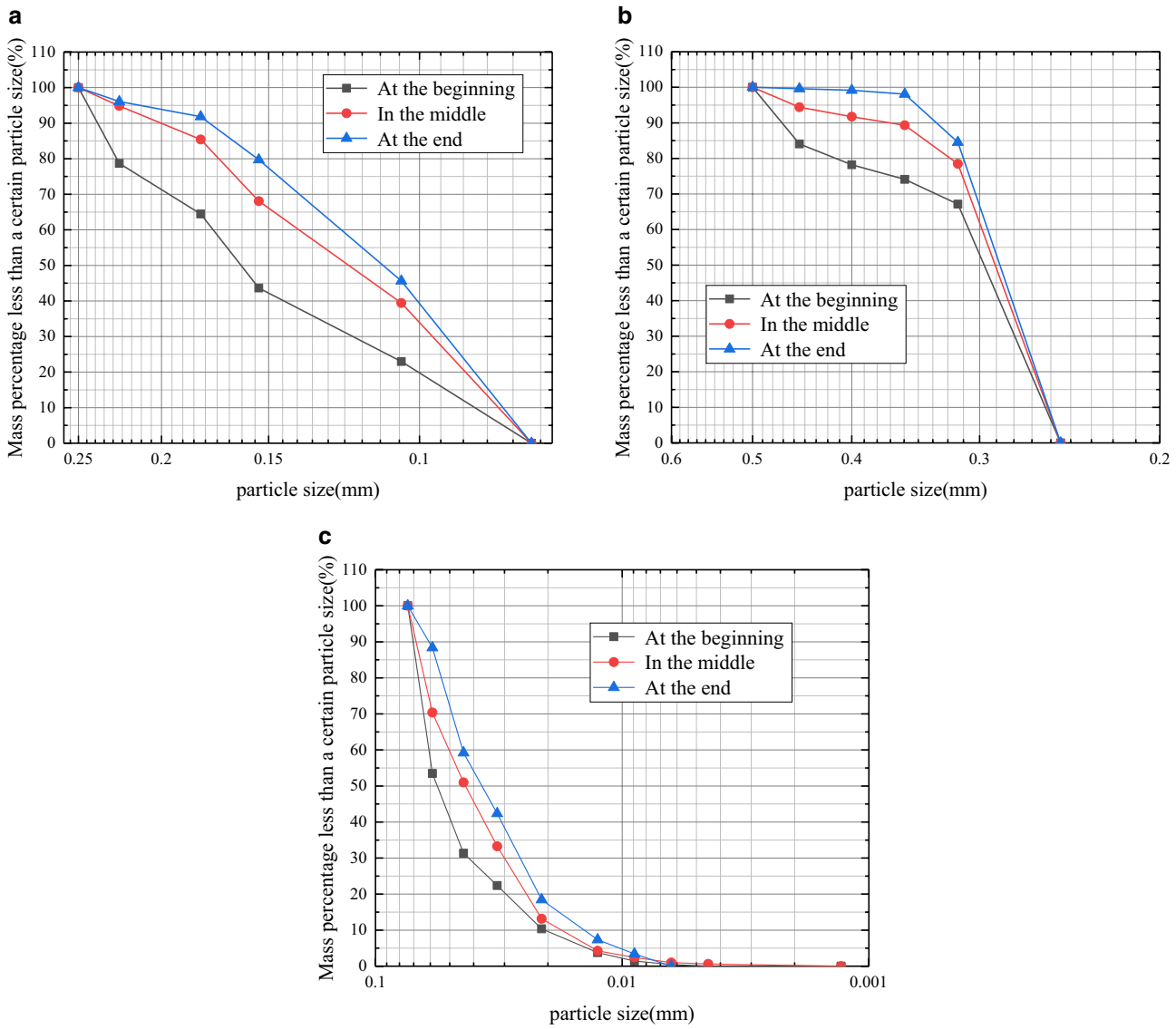

Fig. 11 The granulometry along the length of sedimentation beaches with different particle sizes **a** tailings between 0.074 ~ 0.25 mm; **b** tailings between 0.25 ~ 0.5 mm; **c** tailings < 0.074 mm

Boundary Conditions and Calculation Parameters

According to the relevant parameters of the model test, tailings with different particle sizes and their physical parameters were assigned to the model dam body in the sediment erosion module. The calculation area and boundary conditions of the model are shown in Fig. S-3.

The calculation area was 2.4 m × 0.3 m × 0.27 m (length × width × height), divided into 158,802 numerical grids. The calculated boundary conditions are shown in Supplemental Table S-1. The symmetry boundary (S): fluid velocity, temperature, pressure, and other parameters on the left and right sides of the boundary were distributed symmetrically. Outflow boundary (O): fluid can flow out of the rear boundary of the model dam without backflow. The upper part of the model is the pressure boundary (P): the upper part is a standard atmospheric pressure, and the initial water level upstream of the model was set at 0.158 m. The bottom of the model space was a wall boundary (W), equivalent to the bottom of the glass groove.

The entrainment coefficient and other parameters were automatically calculated by default of the software or obtained by multiple debugging. The parameters are shown in Table 4.

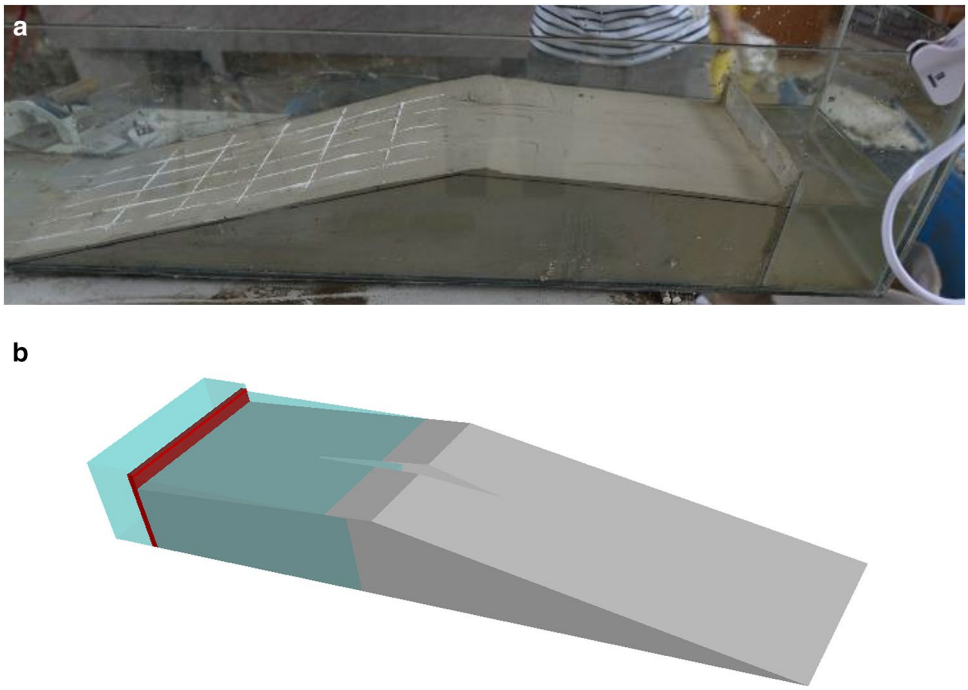

Fig. 12 Schematic diagram of software calculation model **a** model test dam; **b** numerically simulated dam

Numerical Simulation Results

Dam-failure Characteristics

The post-processing part of FLOW-3D was used to describe the dam-break process form (Fig. 13). When the initial gully formed, the collapse began at the foot of the dam body with tailings < 0.074 mm, and a collapsed form of a multi-stage scarp appeared in the gully, which is similar to what occurred in the physical model. For tailings of 0.074 ~ 0.25 mm, the dam body developed a breach in the middle, while the top and toe were not obviously damaged, the breach width was small, and the collapse trend was relatively straight. The 0.25–0.5 mm dam first formed an obvious gully from the top of the dam, and there was a little erosion and accumulation of tailings on the surface of the dam body, while the gully form was roughly like a trumpet, similar what was observed in the model test. However, by default, the tailings have no viscosity in FLOW-3D, so the breach had an inverted triangular cross section, which is inconsistent with the shape of the breach cross section in the physical experiment. Overall, though, the results obtained by numerical simulation and physical experiment were basically similar.

Tailwater Flow Rate

In the numerical simulation, the FLOW-3D software could monitor the tailwater flow through the specified section using a baffle. The results of the software are compared with the results of the physical test in Fig. 14. The time, process, and size of the peak flow determined by numerical simulation and physical experiment agreed well. However, the start of the abrupt flow rate increase appears to start earlier in the initial stage of the dam break in the numerical calculation than in the physical experiment because in the physical tests, water infiltrates into the dam after it begins to overflow, which causes hysteresis of the flow rate.

Duration of the Dam Failure

Accurately understanding the duration of a dam break is of great significance in mitigating tailings reservoir disasters and aiding evacuations, as shown in Table 5. Comparing the results of the physical experiment and numerical simulation, it is found that the durations were similar, which means that the accuracy of the numerical simulation in simulating the duration of the flow is verified. However, the time for the formation of the initial gully was quite different. This may be due to the assumption of uniform particle size in the numerical simulation.

Conclusion

Overtopping is one of the main causes of tailings failure. In this study, the collapse characteristics, flow rate and dam break time of tailings dams with different particle size tailings were systematically studied using laboratory physical model experiments and CFD based numerical simulations. Some conclusions were drawn.

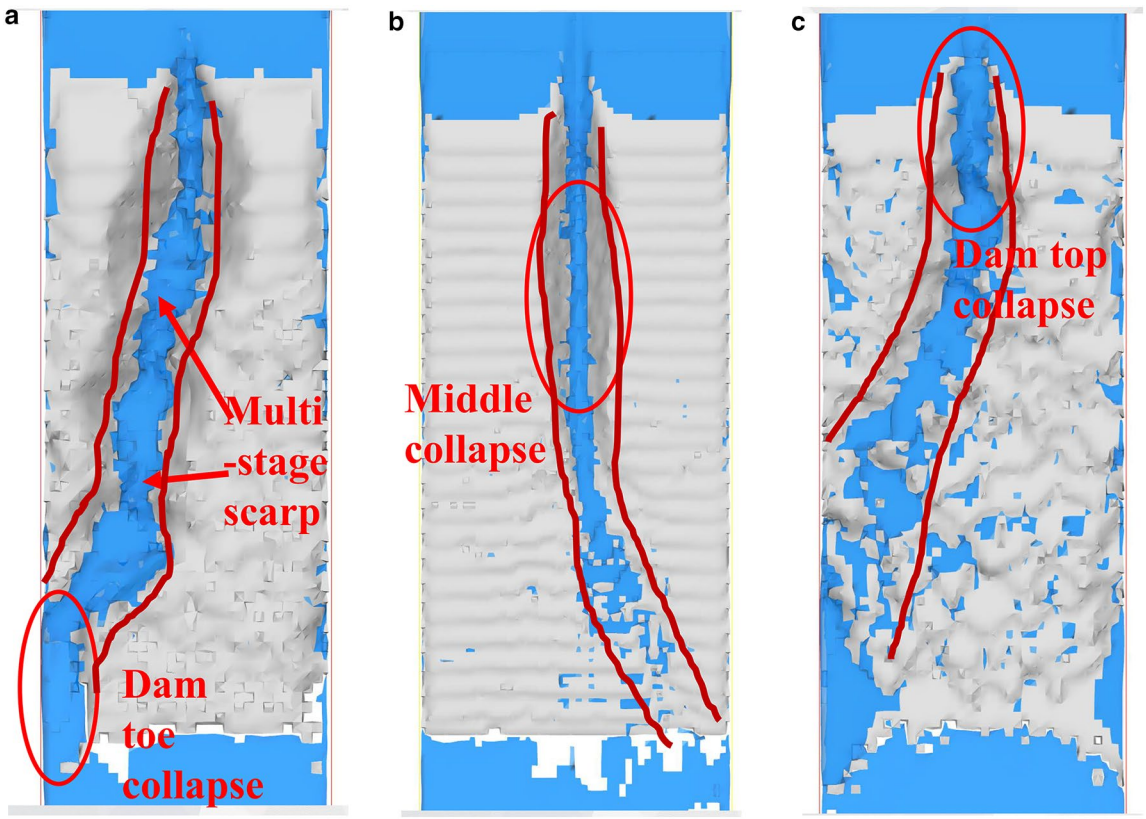

Fig. 13 Breakage morphology from numerical simulation with different particle sizes **a** < 0.074 mm; **b** 0.074 ~ 0.25 mm; **c** 0.25 ~ 0.5 mm

Table 4 Calculation parameters with an angle of repose of 34 and a bedload coefficient of 8

Size (mm)	Diameter (mm)	Density (kg/m^3)	Critical shields number	Entrainment coefficient	Permeability coefficients (m/s)
< 0.074	0.036	3520	0.029	0.0002	0.00001
0.074 ~ 0.25	0.162	3240	0.035	0.0009	0.0002
0.25 ~ 0.5	0.375	2992	0.046	0.0098	0.0004

During the process of dam failures caused by overtopping, no matter the tailings' particle size, the dam will experience the occurrence and development of gullies that deepen and widen with time, until the dam fails.

The size range of the particles affects how the tailings move in the flowing water action, which can lead to two different overtopping failure forms: undercut erosion and surface scouring. Tailings composed of fine particles are mainly characterized by erosion of the dam. Multi-stage and large scarps are prone to occur, and the trajectory of the deep gully that forms is curved.

Tailings dam composed of coarse particles that fail by overtopping are weakened by surface scouring (due to the relatively high bed load). Tailings particles are carried by water for a short distance, and then deposited on the slope of the dam body. The dam body is more permeable, allowing much of the water to flow into the dam.

Tailings dams with medium particle sizes fail due to both undercut erosion (by a relatively straight gully) and surface scouring. The surface of the scouring bed is relatively flat.

Comparing gully formation during the dam-breaking process, we found that the toe of the fine-grained tailings dam collapses first due to undercut erosion. The collapse then develops from toe to the top of the dam. Due to erosion, the gully develops in the form of scarps, which causes the depth of the gully to deepen, until the gully walls on both sides collapse.

Under the action of water flow scouring, the coarse-grained tail sand dam body begins to collapse from the top of the toe. The width of the shallow gully that forms

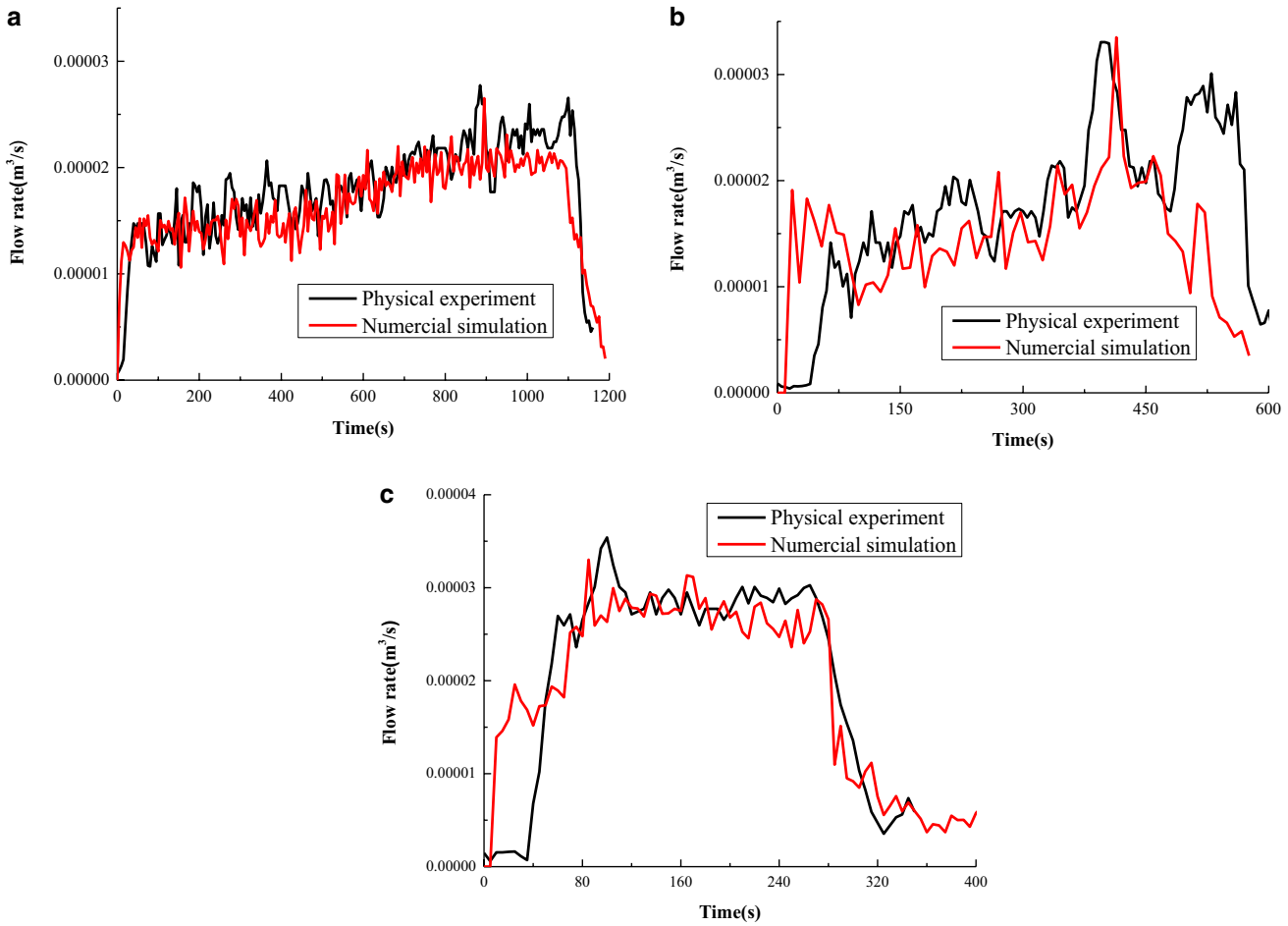

Fig. 14 Comparison between physical experiment and numerical simulation on water flow rates with different particle sizes **a** < 0.074 mm; **b** 0.074 ~ 0.25 mm; **c** 0.025 ~ 0.5 mm

Table 5 Comparison of break duration (unit/s)

Particle size (mm)	State	Physical experiment	Numerical simulation
< 0.074	Initial gully formed	2	355
	Duration of dam break	1314	1295
0.074 ~ 0.25	Initial gully formed	31	200
	Duration of dam break	757	800
0.25 ~ 0.5	Initial gully formed	169	70
	Duration of dam break	513	485

increases from there to the toe of the dam, forming the shape of a horn.

The growth of the gully of the dam with a medium particle size is subtle, and the collapse begins to develop from the middle of the dam. In comparing the width variation of the gully, the development of the gully in the central part of the dam is less at the foot of the dam.

Comparing the physical experiment and numerical simulation results shows that using the numerical method an overtopping tailings dam break is feasible, which can provide ideas and references for other studies on overtopping dam break of tailings pond. Future research will incorporate the effects of chemical reactions and the possible role that the formation of cementitious materials might have on tailings dam failures.

References

Cui Z (1991) China water encyclopedia, vol 3. Water Resources and Electric Power Press, Beijing (**in Chinese**)

Della Vecchia G, Cremonesi M, Pisanò F (2019) On the rheological characterisation of liquefied sands through the dam-breaking test. Int J Numer Anal M Geomech 43(7):1410–1425. https://doi.org/10.1002/nag.2905

Deng Z, Wu S, Fan Z, Yan Z, Wu J (2019) Research on the overtopping-induced breaching mechanism of tailings dam and its numerical simulation. Adv Civil Eng. https://doi.org/10.1155/2019/3264342

Fourie A, Bouazza A, Lupo J, Abrao P (2010) Improving the performance of mining infrastructure through the judicious use of geosynthetics. Proceedings 9th International Conf on Geosynthetics, 193–219

Hanson GJ, Temple DM, Cook KR (1999) Dam overtopping resistance and breach processes research. Proc, Dam Safety. https://www.ars.usda.gov/research/publications/publication/?seqNo115=105272. Accessed 13 Oct 1999

Jeyapalan Jey K, Duncan JM, Seed HB (1983) Investigation of flow failures of tailings dams. J Geotech Eng 109(2):172–189. https://doi.org/10.1061/(ASCE)0733-9410(1983)109:2(172)

Jing X, Chen Y, Williams DJ, Serna ML, Zheng H (2019) Overtopping failure of a reinforced tailings dam: laboratory investigation and forecasting model of dam failure. Water 11(2):315. https://doi.org/10.3390/w11020315

Lyu Z, Chai J, Xu Z, Qin Y, Cao J (2019) A comprehensive review on reasons for tailings dam failures based on case history. Adv Civil Eng 2019:4159306. https://doi.org/10.1155/2019/4159306

Mastbergen DR, Van Den Berg JH (2003) Breaching in fine sands and the generation of sustained turbidity currents in submarine canyons. Sedimentology 50(4):625–637. https://doi.org/10.1046/j.1365-3091.2003.00554.x

Ralston DC (1987) Mechanics of embankment erosion during overflow. Proc Hydraulic Engineering, ASCE 733-738

Rico M, Benito G, Díez-Herrero A (2008) Floods from tailings dam failures. J Hazard Mater 154(1):79–87. https://doi.org/10.1016/j.jhazmat.2007.09.110

Schmocker L (2009) The failure of embankment dams due to overtopping. J Hydraul Res 47(2):288–288. https://doi.org/10.1080/00221686.2009.9521999

Soulsby R (1998) Bedload transport dynamics of marine sand, Ch. 9. Thomas Telford Publ, London, pp 155–170

Sun E, Zhang X, Li Z, Wang Y (2012) Tailings dam flood overtopping failure evolution pattern. Procedia Eng 28:356–362. https://doi.org/10.1016/j.proeng.2012.01.733

Sun R, Wang X, Zhou Z, Ao X, Sun X, Song M (2014) Study of the comprehensive risk analysis of dam-break flooding based on the numerical simulation of flood routing Part I: model development. Nat Hazards 73(3):1547–1568. https://doi.org/10.1007/s11069-014-1154-z

Tabri K, Määttänen J, Ranta J (2008) Model-scale experiments of symmetric ship collisions. J Mar Sci Technol 13(1):71–84. https://doi.org/10.1007/s00773-007-0251-z

Wahl TL (1998) Prediction of embankment dam breach parameters - a literature review and needs assessment. U.S. Dept. of the Interior, Bureau of Reclamation, Dam Safety Report DSO-98-004, Denver, CO

Wilcox D (1994) Turbulence Modeling for CFD. DCW Industrie Inc, Canada

Wu J, Wu Y, Lu J (2008) Laboratory study of the clogging process and factors affecting clogging in a tailings dam. Environ Geol 54(5):1067–1074. https://doi.org/10.1007/s00254-007-0873-9

Wu T, Qin J (2018) Experimental study of a tailings impoundment dam failure due to overtopping. Mine Water Environ 37(2):272–280. https://doi.org/10.1007/s10230-018-0529-x

Yin G, Li G, Wei Z, Wan L, Shui G, Jing X (2011) Stability analysis of a copper tailings dam via laboratory model tests: a Chinese case study. Miner Eng 24(2):122–130. https://doi.org/10.1016/j.mineng.2010.10.014